

Particle Scattering in the Resonance Regime: Models Based on Integral Equations and Hybrid Finite Elements - Integral Equation Techniques

Cinzia Zuffada and David Crisp

Jet Propulsion Laboratory, California Institute of Technology
Pasadena, CA 91109
cinzia@yellowstone.jpl.nasa.gov dc@crispy.jpl.nasa.gov

ABSTRACT

Reliable descriptions of the optical properties of clouds and aerosols are essential for studies of radiative transfer in the terrestrial atmosphere. Mie scattering algorithms provide accurate estimates of these properties for spherical particles with a wide range of sizes and refractive indices, but these methods are not valid for non-spherical particles. Even though a host of methods exist for deriving the optical properties of non-spherical particles that are very small, or very large compared to the wavelength, only a few methods are valid in the resonance regime, where the particle dimensions are comparable to the wavelength. Most such methods are not ideal for particles with sharp edges or large axial ratios. Here, we explore the utility of two approaches for deriving the single scattering optical properties of particles with sharp corners and large axial ratios. The first is a surface integral equation for axisymmetric particles; the second is a hybrid finite element-integral equation approach, suitable for particles of arbitrary shape, possibly inhomogeneous and anisotropic. We derive cross sections, single scattering albedos, and phase functions, for ice cylinders, prisms and disks with dimensions extending from the Rayleigh to the geometric optics regimes. Our results show that water ice disks and cylinders are more strongly absorbing than equivalent volume spheres at most infrared wavelengths. The geometry of these particles also affects the angular dependence of the scattering. Disks and columns with maximum linear dimensions larger than the wavelength scatter much more radiation in the forward and backward directions, and much less at intermediate phase angles than equivalent volume spheres.

Key words: clouds and aerosols, axis-symmetric particles, resonance regime.

SECTION I

Non-spherical aerosol particles play an important role in the radiation budgets of planetary atmospheres. For example, cirrus clouds in the Earth's upper

troposphere reduce the solar input to the climate system by reflecting sunlight to space before it can be absorbed, and act as greenhouse agents by trapping thermal radiation emitted by the surface and lower troposphere. However, the net radiative forcing by cirrus clouds depends critically on the microphysics and wavelength-dependent optical properties assumed for the ice particles. Existing observations indicate that these clouds consist primarily of hexagonal columns, plates, and rosettes, with a wide range of aspect ratios and dimensions ranging from a few microns to several hundred microns. Reliable estimates of the wavelength-dependent optical properties of non-spherical aerosols are essential for the retrieval of their abundances and distributions from remote sensing observations. This information is also needed in climate models to estimate their contributions to the solar and thermal radiative forcing. These calculations are particularly demanding because they require accurate estimates of the particle optical properties over a wide range of sizes at wavelengths extending from the far ultraviolet (0.1 μm) to the far infrared (250 μm).

A variety of analytical models are available for particle sizes that are smaller than or equal to one wavelength (Rayleigh regime). These methods are summarized by van de Hulst (1957). The Discrete Dipole Approximation (Purcell and Pennypacker, 1973; Draine, 1988) belongs in this category, since it calculates the scattering from an arbitrary object by replacing it with an array of discrete elementary electric dipoles, interacting with each other, and the electric dipole moments of the source distribution are then calculated. This method has been used to calculate optical properties of aggregate particles of arbitrary shape, with sizes comparable to about one wavelength (West, 1991). The Finite Difference Time Domain approach was used by Tang and Aydin (1995) to model ice crystals in the millimeter wave range. This method, which solves Maxwell's equations in differential form, can model arbitrary shapes by step-wise approximations. This is a full wave method, although the step size can become a limiting factor in the model fidelity.

Methods based on integral equations (full-wave analysis) have also received attention. The approach, in principle exact, does not have any particle size

limitations, although general three-dimensional volumetric integral equations are difficult to implement. One particular formulation of a surface integral equation, the Extended Boundary Condition (EBC) method, based on the enforcement of the extinction theorem, has proven successful for modeling of spheroids and cylinders (Barber and Yeh, 1972; Mishchenko, 1991; Kuik et al., 1992; Kuik et al., 1994). This method makes use of expansions of the fields in series containing spherical harmonics. It is most efficient for calculating the optical parameters of ensembles of randomly oriented particles, since angular integrations for orientational averages can be performed analytically. However, for scatterers with large axial ratios and/or with sharp corners, the resulting matrices' condition numbers can become large (Kuik et al., 1994; Ishimaru, 1991). A surface integral equation technique for axisymmetric scatterers has been known in the microwave community for some years, to model scattering from bodies with sharp edges and points (Medgeysi-Mitschang and Putnam, 1984). Finite elements have been adopted more recently to model scattering from penetrable, inhomogeneous bodies of general shape (Cwik et al., 1996). In this last method the features of the scatterers can be modeled accurately on the scale of a fraction of the wave length. In our work we have applied these techniques to calculations of optical properties of ice disks, cylinders and hexagonal prisms with aspect ratio of 10.

SECTION II

IIa. SURFACE INTEGRAL EQUATION FOR AXISYMMETRIC PARTICLES

We define fictitious electric ($\vec{J} = \hat{n} \times \vec{H}$) and magnetic ($\vec{M} = -\hat{n} \times \vec{E}$) surface currents, equivalent to the tangential magnetic and electric fields on the exterior surface of the scatterer. The scattered fields are obtained from the tangential currents via an integral over the boundary using the free-space Green's function kernel. A linear combination of the electric field integral equation (EFIE) and the magnetic field integral equation (MFIE) yields the general form

$$Z_m[\vec{M}/\eta_0] + Z_e[\vec{J}] = V_i$$

where Z_m and Z_e are the integro-differential operators used in defining the EFIE, and V_i represents the incident field. Orthogonal surface coordinates (t, ϕ) are used on the surface of revolution (SOR); ϕ is the azimuthal angle variable and t is the contour length variable along the SOR generating curve. Using the method of moments, this integral equation is turned into a matrix

equation. Note that the representations for the unknown surface currents are separable in the two surface coordinates, and the azimuthal Fourier modes are orthogonal. This results in impedance matrices which are only block-diagonal, as opposed to the completely full matrices for general surface integral equations. Storage requirements are thus reduced, as well as fill and solution times.

IIb. HYBRID FINITE ELEMENTS - INTEGRAL EQUATION TECHNIQUE

We apply the finite element technique in a volume containing the particle and a portion of the medium around it up to a mathematical surface of revolution (SOR). Here an integral equation is set up for the equivalent electric and magnetic surface currents, thus enforcing an exact boundary condition at the truncation of the computational domain. A finite element discretization of an integral form of the wave equation is used for the unknown fields in the volume. Applying a form of Green's theorem, a weak form of the wave equation is obtained, which includes a surface integral. This provides for a boundary condition relating the field inside the selected volume to the field on the boundary, and thus establishes a link to the outside field. Furthermore, a set of unknown surface current densities is introduced on the surface, which give rise to the scattered fields. This step leads to an equation which is formally analogous to the EFIE outlined above. Finally, a third equation is introduced by imposing the continuity of the tangential component of the unknown fields at the boundary surface. Compared to a volume EFIE, the finite element technique yields problem matrices which are very sparse. This results in comparative savings in required storage.

SECTION III

We have performed extensive calculations with our surface integral equation code for axisymmetric particles, modeling cylinders, disks and spheroids. On the other hand, we have obtained only a limited amount of results for small hexagonal prisms using the hybrid finite elements - integral equation technique. For this reason, and because of limited space, in this paper we are reporting results obtained with the first technique only.

We considered an ensemble of right circular ice cylinders, arbitrarily oriented in the x-y (azimuthal) plane of a Cartesian coordinate system. This system represents the laboratory fixed frame, and the direction of the incoming light is allowed to vary. The aspect ratio (height/diameter) was fixed at 10 and the wavelength for the incident light was 1 μm . Cylinders' heights of 20 wavelengths were considered to show the applicability of the surface integral equation technique, to a broad range of

particle sizes, bridging the Rayleigh scattering to geometric optics regimes. Figure 1 illustrates the phase function, for 3 different angles of incidence. The results are contrasted with the phase function of the equivalent volume sphere, obtained with a Mie scattering code. Note that ensembles of cylinders and equivalent volume spheres have significantly different phase functions. The peak in the backscattering direction, noticeable at incidence zenith angle of 180 degrees, is the most significant difference from the scattering of an equivalent volume sphere, apart from different resonant features at intermediate zenith angles.

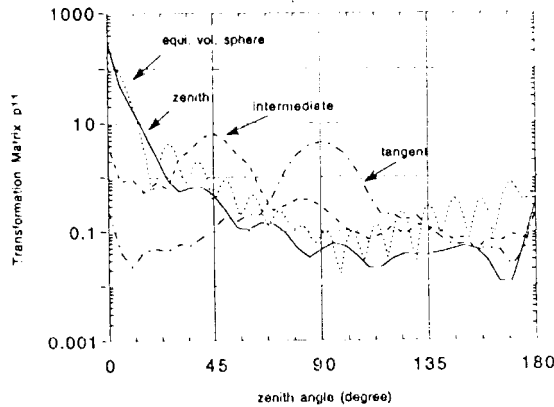


Figure 1. Transformation Matrix p_{11} for ensemble of ice cylinders (height/diameter = 10) arbitrarily oriented in the horizontal plane. $\lambda = 1 \mu\text{m}$, cylinder height = 20λ .

The enhanced backscattering peak is due to the larger surface area presented by the cylinder ensemble compared to a sphere, and the different paths for wave propagation inside the scatterers. For angles of incidence varying between 180, 135 and 90 degrees, the forward scattering peaks broaden, and their intensities decrease as the illumination angle approaches 90 degrees. Indeed the light paths inside, and about the scatterers as a function of incidence angle are very different from one another, unlike for a sphere. These results suggest that the variation in the scattering phase function and the associated illumination-angle-dependent extinction cross sections provide constraints on the scatterer shape for particles in this size range.

Next, we considered ice disks, oriented in the plane x-y with their aspect ratio (height/diameter) fixed at 0.1. The same wavelength was considered as above. Disks diameters of 20 wavelengths were used in the calculations. Hence, the results presented in Figure 2 can be compared to those of Figure 1.

For a disk with a diameter of 20 wavelengths, a very strong backscattering peak is observed. The value of this peak is at least two orders of magnitude higher than that for an equivalent volume sphere. Indeed, additional calculations not reported here show that the overall

angular dependence of p_{11} varies with wavelength only in a region around 90 degrees, where the overall field values are several orders of magnitude smaller than in the forward scattering direction. The strong backscattering peak occurs for scatterers with large flat surfaces and parallel planes resulting in strong reflection. The behavior of p_{11} as a function of direction of the incident light exhibits more narrow peaks than the correspondent curves for cylinders. Backscattering for the intermediate direction is more pronounced than for the cylinders, since the cylinders' curved surfaces cause different diffraction and reflection paths from the disk's parallel planes.

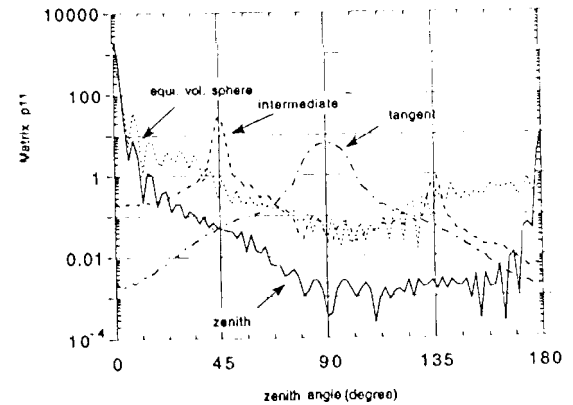


Figure 2. Transformation Matrix p_{11} for ice disk (height/diameter = 0.1) laying in the horizontal plane. $\lambda = 1 \mu\text{m}$, disk diameter = 20λ .

In addition to phase functions, wavelength-dependent single scattering albedos were calculated for one particle size, at selected wavelengths between 0.1 and $10 \mu\text{m}$. We considered fairly small particles with maximum dimensions $10 \mu\text{m}$. Hence, the smallest wavelength used for these calculations was one tenth of the maximum dimension. Results are displayed in Figure 3 for cylinder ensembles, and in Figure 4 for the disk. These single scattering albedos were ratioed to the corresponding albedos of equivalent volume spheres.

Several features are worth noting. First, the albedo of cylinders and disks is noticeably smaller than that of spheres at wavelengths between 2 and $10 \mu\text{m}$, where ice has appreciable absorption, whereas it is very close to that of spheres for wavelengths between 0.1 and $1 \mu\text{m}$, where absorption is very small. At the shortest wavelengths, non-spherical particles have higher single scattering albedos than spheres, although this trend might be a fairly localized behavior.

In fact, in the very high frequency (large particle) limit the scattering efficiency of any particle tends to 2, and therefore the ratio tends to 1. Similarly, at the very low frequency limit, the albedo of any lossy particle tends to $O(\sim \lambda^{-4})$, and the ratio will still attain the value of 1. In the region of very low absorption (order 10^{-6} and

lower), albedos will tend to be very close to 1 for any particle shape, and thus the albedo ratio will not vary appreciably with shape. On the other hand, the most interesting regions are those where some absorption is present and the particle size is neither too small nor too large. It is here that the dependence on shape is most pronounced, as shown in Figures 3 and 4.

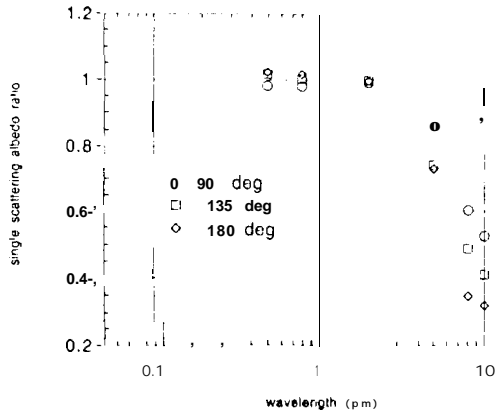


Figure 3. Single scattering albedo, ratioed to equivalent volume sphere, for ensemble of ice cylinders (height/diameter = 10) arbitrarily oriented in the horizontal plane. Cylinder height = 10 μm .

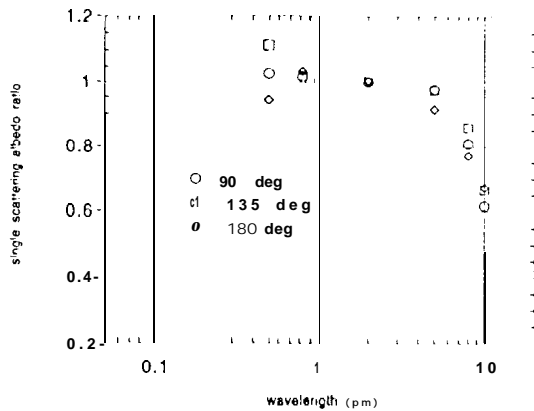


Figure 4. Single scattering albedo, ratioed to equivalent volume sphere, for ice disks (height/diameter = 0.1) laying in the horizontal plane. Disk diameter = 10 μm .

In particular, our results imply that particles with large aspect ratios, oriented in a horizontal plane, have very different albedos in the resonant regime from spheres. This effect could lead to overestimates in the retrieved optical thicknesses of these particles if they were, assumed to be spheres or low-aspect-ratio spheroids. The size of such errors depends on the size distributions being considered. Additional calculations, not reported here, show that it could be around 50% for the range 1 to 10 μm .

REFERENCES

- Barber, P. W., and C. Yeh, Scattering of electromagnetic waves by arbitrary shaped dielectric bodies, *Appl. Opt.*, 14, 2864-2872, 1972.
- Cwik, T., C. Zuffada, and V. Jamnejad, "Modeling Three-Dimensional Scatterers Using a Coupled Finite Elements - Integral Equation Formulation, *IEEE Trans. AP - S*, pp. 453-459, Apr. 1996.
- Draine, B.T., The discrete dipole approximation and its application to interstellar graphite grains, *Astrophys. J.*, 333, 848-872, 1988.
- van de Hulst, H. C., *Light scattering by small particles*, (John Wiley & Sons, N. Y., 1957).
- Ishimaru, A., *Electromagnetic wave propagation, radiation and scattering*, (Prentice Hall, N. J., 1991), Chap. 12, p. 354.
- Kuik, F., de Haan, J.F., and J.W. Hovenier, Benchmark results of single scattering by spheroids, *J. Quant. Spectrosc. Radiat. Transfer*, 47, 477-489, 1992.
- Kuik, F., de Haan, J. F., and J.W. Hovenier, Single scattering of light by circular cylinders, *App. Optics*, 33, 4906-4918, 1994.
- Medgeysi-Mitschang, I. N., and J.M. Putnam, Electromagnetic scattering from axially inhomogeneous bodies of revolution, *IEEE Trans. on Antennas and Propagation*, 32, 797-806, 1984.
- Mishchenko M. I., T-matrix computations of light scattering by large spheroidal particles, *J. Opt. Soc. Am. A*, 8, 871-882, 1991.
- Purcell, E.M., and C.R. Pennypacker, Scattering and absorption of light by nonspherical dielectric grains, *Astrophys. J.*, 186, 705-714, 1973.
- Tang, C. and K. Aydin, Scattering from ice crystals at 94 and 220 millimeter wave frequencies, *IEEE Trans. Geosci. Remote Sensing*, 33, 93-99, 1995.
- West, R. A., Optical properties of aggregate particles whose outer diameter is comparable to the wavelength, *Appl. Opt.*, 30, 5316-5324, 1991.